Regularity of Radon Transform on a Convex Shape

Pat Vatiwutipong[*]

Department of Mathematics and Computer Science, Kamnoetvidya Science Academy, Rayong, 21210, Thailand

A R T I C L E   I N F O

A B S T R A C T

Radon transform is a mathematical tool widely applied in various domains, including biophysics and computer tomography. Previously, it was discovered that applying the Radon transform to a binary image comprising circle forms resulted in discontinuity. As a result, the line detection approach based on it became discontinued. The d-Radon transform is a modified version of the Radon transform that is presented as a solution to this problem. The properties of the circle cause the Radon transform to be discontinuous. This work extends this finding by looking into the Radon transform's regularity property and a proposed modification to a convex shape. We discovered that regularity in the Radon space is determined by the regularity of the shape's point. This leads to the continuity condition for the line detection method.

1 Introduction

This paper is an extension of work originally presented in the 2022 14th International Conference on Knowledge and Smart Technology (KST) [1].

Radon transform is a well-known integral transform used in many fields that was originally invented in 1917 by Johann Radon, [2]. The Radon is used to create an image from the projection data associated with cross-sectional scans, [3]. Many other integral transforms, such as the Hough transform, Penrose transform, and Fourier transform, are significantly associated with the Radon transform.

Intuitively, Radon transformation is to integrate a given object and project the value onto the lower-dimensional space in various directions. In computer tomography, for example, the Radon transform was applied to a 3D object to obtain a 2D image. In practice, we acquire the 2D projected picture and must use the inversion of the Radon transform to reconstruct the 3D object, [4].

Hough transform is one of the line detection techniques used in image processing. By applying the Hough transform to an image, the image's point accumulation in each direction is computed. In the Hough space, a direction that passes through more points will have a greater value if the image comprises multiple points. The line direction in the image can be used to detect the maximal argument on the Hough space, [5].

In 2016, the author found a unifying perspective of the Radon and Hough transformations [6]. The Radon transform is considered a continuous version of the Hough transform, so it was also applicable as a line detection method by changing the accumulation function to the integration of images in each direction instead. Since the Hough transform is a discrete transformation, the line detection method's continuity cannot be expected. However, it is different for the Radon transform.

In [1], we explained the benefits of the continuity of line detection method. It has been shown that the continuity of the line detection method using Radon transform depends on the regularity of the Radon space, but that work focused only on the image containing points. In practice, an actual image contains not only points but also shapes. For a grey-scale image as a function from a 2D image space to the interval [0, 1], the value 0 and 1 represent white and black colors, respectively. If the image is continuous, we have that the Radon transform is also continuous. Nevertheless, image discontinuity is expected for a binary image whose range is just {0, 1}. This paper aims to study the regularity properties of the Radon transform of a binary image containing shapes, which lead to the continuity of the line detection method.

2 Definition and Elementary Properties

This section presents the definition of *Radon transform* and its basic properties.

Definition 2.1. (Radon transform) For a given function $m : W \subset \mathbb{R}^2 \to \mathbb{R}$, the Radon transform of m is defined, for each pair of real numbers θ and r,

$$\mathcal{R}[m](\theta, r) = \int_{r=x\cos\theta+y\sin\theta} m(x, y)ds, \tag{1}$$

[*]Corresponding Author: Pat Vatiwutipong, Email: pat.v@kvis.ac.th

whenever the integration is defined.

Lemma 2.2. *We have $(x, y) \in \ell_{\theta,r}$ if and only if there exists $s \in \mathbb{R}$ satisfying $x = r\cos\theta - s\sin\theta$ and $y = r\sin\theta + s\cos\theta$.*

According to this lemma, we can rewrite the definition of Radon transform as

$$\mathcal{R}[m](\theta, r) = \int_{-\infty}^{\infty} m(r\cos\theta - s\sin\theta, r\sin\theta + s\cos\theta)ds. \quad (2)$$

It was proven in [7] that the Radon transform $\mathcal{R}[m]$ exists for all $m \in L^1(\mathbb{R}^2)$.

For a function $h : E \to \mathbb{R}$, define a *norm* as in [7] by,

$$\|h\|_{\infty,1} = \max_{\theta \in [-\frac{\pi}{2}, \frac{\pi}{2})} \int_{-\infty}^{\infty} |h(\theta, r)|dr. \quad (3)$$

It was also proven in [7] that, for $m \in L^1(\mathbb{R}^2)$,

$$\|\mathcal{R}[m]\|_{\infty,1} \le \int_{\mathbb{R}^2} |m(x, y)|dxdy. \quad (4)$$

Since the Radon transform is linear, we have

$$\|\mathcal{R}[m] - \mathcal{R}[\tilde{m}]\|_{\infty,1} \le \int_{\mathbb{R}^2} |m(x, y) - \tilde{m}(x, y)|dxdy, \quad (5)$$

which means that if there is a small change on the function m, the change on its Radon transform will also be small.

3 Regularity of Radon Transform

3.1 Regularity on Circle

First, let B_1 be a single circle in image space W centered at $P_1 = (x_1, y_1)$ with radius $R_1 > 0$. The Radon transform of this single circle is equal to the length of the intersection between the circle and $\ell_{\theta,r}$, so if the circle is centered at the origin, we have that

$$\mathcal{R}[B_1](\theta, r) = \begin{cases} 2\sqrt{R_1^2 - r^2} & \text{if } |r| \le R_1 \\ 0 & \text{otherwise.} \end{cases} \quad (6)$$

Linearity and shifting property of the Radon transform are proven in [8]. From the shifting property,

$$\mathcal{R}[B_1](\theta, r) = \begin{cases} 2\sqrt{R_1^2 - (r - x_1\cos\theta - y_1\sin\theta)^2} \\ \qquad \text{if } |r - x_1\cos\theta - y_1\sin\theta| \le R_1 \\ 0 \qquad \text{otherwise.} \end{cases} \quad (7)$$

Recall that we can represent $\mathcal{R}[P_1](\theta, r)$ by a sinusoidal curve $r_1(\theta) = x_1\cos\theta + y_1\sin\theta$, so we have that

$$\mathcal{R}[B_1](\theta, r) = \begin{cases} 2\sqrt{R_1^2 - (r - r_1(\theta))^2} & \text{if } |r - r_1(\theta)| \le R_1 \\ 0 & \text{otherwise.} \end{cases} \quad (8)$$

In the Radon space E, the graph of $\mathcal{R}[B_1](\theta, r)$ can be seen as a "tunnel" centered at r_1 (see Figure 1).

When θ is fixed we can consider $\mathcal{R}[B_1](\theta, r)$ as a function of r which forms an upper-half of an ellipse centered at $r_1(\theta)$, with base length and height equal to $2R_1$ (see figure 2).
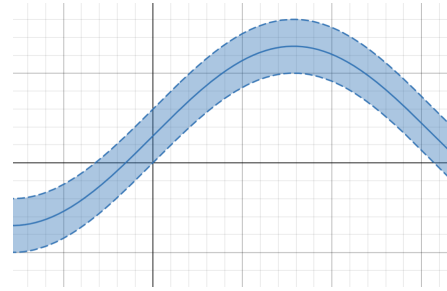

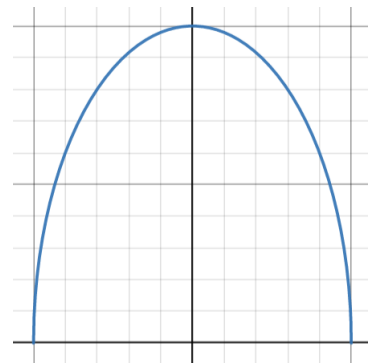Figure 1: Graph of $\mathcal{R}[B_1](\theta, r)$ in E

Figure 2: Cross section of $\mathcal{R}[B_1](\theta, r)$ for a fixed θ.

In this setting, the Radon transform $\mathcal{R}[B_1](\theta, r)$ is a continuous function on (θ, r) but it is not differentiable in r at $r = r_1(\theta) \pm R$.

To obtain more regularity, we modify the Radon transform by changing the integration domain from a line to a strip centered at that line instead.

Definition 3.1. (*d*-Radon transform) For $d > 0$ and $m \in L^1(\mathbb{R}^2)$, define the $d-$Radon transform of m, for each pair of real numbers θ and r, by

$$\mathcal{R}_d[m](\theta, r) = \int_{r-d}^{r+d} \mathcal{R}[m](\theta, \rho)d\rho. \quad (9)$$

We also have linearity and shifting properties for our new transformation. By the fundamental theorem of calculus and the fact that $\mathcal{R}[B_1](\theta, r)$ is continuous, the d-Radon transform $\mathcal{R}_d[B_1](\theta, r)$ is differentiable in r. Next, we will derive $\mathcal{R}_d[B_1](\theta, r)$ explicitly for each θ. For the sake of convenience, we shift the Radon space such that $r_1(\theta) = 0$. We have two cases.

Case I: If $0 < d \le R_1$, we have that

$$\mathcal{R}_d[B_1](\theta, r) = \begin{cases} \int_{r-d}^{R_1} \mathcal{R}[B_1](\theta, \rho)d\rho & \text{if } R_1 \le r \le R_1 + d \\ \int_{r-d}^{r+d} \mathcal{R}[B_1](\theta, \rho)d\rho & \text{if } -R_1 \le r \le R_1 \\ \int_{-R_1}^{r+d} \mathcal{R}[B_1](\theta, \rho)d\rho & \text{if } -R_1 - d \le r \le -R_1. \end{cases}$$

That is $\mathcal{R}_d[B_1](\theta, r)$

$$
= \begin{cases}
\frac{\pi R_1^2}{2} - [(r-d)\sqrt{R_1^2 - (r-d)^2} + R_1^2 \arctan(\frac{r-d}{\sqrt{R_1^2 - (r-d)^2}})] \\
\qquad \text{if } R_1 \leq r \leq R_1 + d \\
[(r+d)\sqrt{R_1^2 - (r+d)^2} + R_1^2 \arctan(\frac{r+d}{\sqrt{R_1^2 - (r+d)^2}})] \\
\quad -[(r-d)\sqrt{R_1^2 - (r-d)^2} + R_1^2 \arctan(\frac{r-d}{\sqrt{R_1^2 - (r-d)^2}})] \\
\qquad \text{if } -R_1 \leq r \leq R_1 \\
\frac{\pi R_1^2}{2} + [(r+d)\sqrt{R_1^2 - (r+d)^2} + R_1^2 \arctan(\frac{r+d}{\sqrt{R_1^2 - (r+d)^2}})] \\
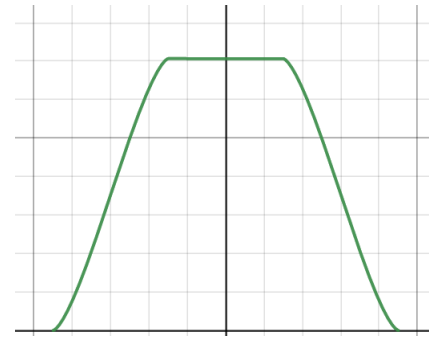\qquad \text{if } -R_1 - d \leq r \leq -R_1.
\end{cases}
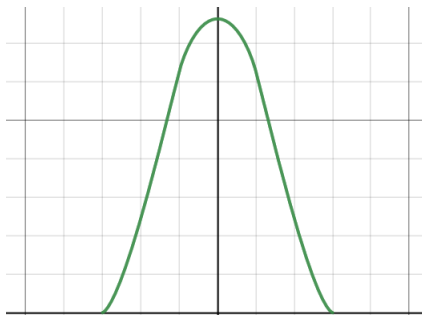\tag{10}
$$

The graph is shown in Figure 3.

Figure 3: Cross section of $\mathcal{R}[B_1]_d(\theta, r)$ when $0 < d \leq R_1$ for a fixed θ.

<u>Case II:</u> If $R_1 < d$, we have that

$$
\mathcal{R}_d[B_1](\theta, r) = \begin{cases}
\int_{r-d}^{R_1} \mathcal{R}[B_1](\theta, \rho) d\rho & \text{if } R_1 \leq r \leq R_1 + d \\
\int_{-R_1}^{R_1} \mathcal{R}[B_1](\theta, \rho) d\rho & \text{if } -R_1 \leq r \leq R_1 \\
\int_{-R_1}^{r+d} \mathcal{R}[B_1](\theta, \rho) d\rho & \text{if } -R_1 - d \leq r \leq -R_1.
\end{cases}
$$

That is $\mathcal{R}_d[B_1](\theta, r)$

$$
= \begin{cases}
\frac{\pi R_1^2}{2} - [(r-d)\sqrt{R_1^2 - (r-d)^2} + R_1^2 \arctan(\frac{r-d}{\sqrt{R_1^2 - (r-d)^2}})] \\
\qquad \text{if } R_1 \leq r \leq R_1 + d \\
\pi R_1^2 \qquad \text{if } -R_1 \leq r \leq R_1 \\
\frac{\pi R_1^2}{2} + [(r+d)\sqrt{R_1^2 - (r+d)^2} + R_1^2 \arctan(\frac{r+d}{\sqrt{R_1^2 - (r+d)^2}})] \\
\qquad \text{if } -R_1 - d \leq r \leq -R_1.
\end{cases}
\tag{11}
$$

The graph is shown in Figure 4.

Figure 4: Cross section of $\mathcal{R}[B_1]_d(\theta, r)$ when $R_1 < d$ for a fixed θ.

For a fixed θ, $\mathcal{R}[B_1](\theta, r)$ reaches its maximum at $r = r_1(\theta)$. If $d \leq R_1$, the maximum is $2d\sqrt{R_1^2 - d^2} + 2R_1^2 \arctan(\frac{d}{\sqrt{R_1^2 - d^2}})$ and if $d > R_1$, the maximum is πR_1^2.

Lemma 3.2. *Let B_1 and B_2 be circles with same radius R, and fix $\theta \in [-\frac{\pi}{2}, \frac{\pi}{2})$, we have that*

$$
\max_{r \in \mathbb{R}} |\mathcal{R}[B_1](\theta, r) - \mathcal{R}[B_2](\theta, r)| = \min\{2R, 2\sqrt{2Ra_\theta - a_\theta^2}\}
\tag{12}
$$

and

$$
\max_{r \in \mathbb{R}} |\mathcal{R}_d[B_1](\theta, r) - \mathcal{R}_d[B_2](\theta, r)| \leq 2\sqrt{2}Ra_\theta
\tag{13}
$$

where $a_\theta = |r_1(\theta) - r_2(\theta)|$.

Proof. The proof of this lemma is straightforward. $\qquad\square$

Now, we define another norm for the Radon space.
For a function $h : E \to \mathbb{R}$ define

$$
\|h\|_\infty = \max_{(\theta, r) \in [-\pi, \pi) \times \mathbb{R}} |h(\theta, r)|.
\tag{14}
$$

Let B_1 be a circle and B_2 be another circle obtained by shifting B_1 with distance δ. We have that the value of $|\mathcal{R}[B_1](\theta, r) - \mathcal{R}[B_2](\theta, r)|$ will reach the maximum when $a_\theta = \|P_1 - P_2\| = \delta$. So, from Lemma 3.2, we get that $\|\mathcal{R}[B_1] - \mathcal{R}[B_2]\|_\infty = \min\{2R, 2\sqrt{2R\delta - \delta^2}\}$ which cannot be bounded by $C\delta$ for any constant C. Indeed, its derivative when δ is close to zero tends to infinity. So, in this case, a small change in the image will create a large change in its Radon transform.

For the d-Radon transform, the situation is totally different. Since we have a linear estimation in the previous lemma, we get that $\|\mathcal{R}_d[B_1] - \mathcal{R}_d[B_2]\|_\infty \leq 2\sqrt{2}R\delta$. By linearity of d-Radon transform, we can extend this result to the case of images containing more than one circle. This leads to the next proposition.

Definition 3.3. Let $\mathfrak{B}$ be a set of all images containing a finite number of circles with the same radius $R > 0$. Define a distance function $\bar{D}$ on $\mathfrak{B}$ by $\bar{D}(m_1, m_2) = \bar{d}(m_1^P, m_2^P)$ where $\bar{d}$ is defined in Equation (4) and m^P is an image containing only the center of each circle in m.

Proposition 3.4. *Let $m_1, m_2 \in \mathfrak{B}$ be two images which contain N_1 and N_2 circles respectively, and $N_M = \max\{N_1, N_2\}$. We have that*

$$
\|\mathcal{R}_d[m_1] - \mathcal{R}_d[m_2]\|_\infty \leq 2\sqrt{2}RN_M\bar{D}(m_1, m_2).
\tag{15}
$$

3.2 Regularity on Convex Shape

Let m be an image that contains a single convex shape, that is, $m(x, y) = 1_A$, where A is a connected, compact and convex subset of W. Let curve C be the boundary of A. Suppose that C is continuous and piecewise differentiable.

Definition 3.5. Let P be a point on C. Let $\partial C(P)$ be the set of $\phi \in [-\pi, \pi)$ such that there exists r_ϕ which makes line $\ell_{\phi, r_\phi} : r_\phi = x \cos \phi + y \sin \phi$ intersects the set C only at point P or tangent of C in P.

Note that $\partial C(P)$ always exists for any P since C is convex, and it is a singleton when P is a differentiable point of C.

Remark 3.6. Since C is a closed curve, we get that the set $\{\phi : \phi \in \partial C(P), P \in C\}$ is equal to $[-\pi, \pi)$.

For all $\phi \in \partial C(P)$, let $\ell_{\phi, r_\phi}^\perp$ be the perpendicular line to ℓ_{ϕ, r_ϕ} passing through P. Denote the length of the segment of $\ell_{\phi, r_\phi}^\perp$ that intersected with A by D_ϕ. Parameterize $\ell_{\phi, r_\phi}^\perp$ by s. Set s to be zero at P and $s > 0$ in the direction that passes through A.

Definition 3.7. For a fixed P, define a function $f_\phi : \mathbb{R} \to \mathbb{R}$, for each ϕ, by letting $f_\phi(s)$ be the length of $\ell_{\phi, r_\phi + s}$ across A. Equivalently, $f_\phi(s) = \mathcal{R}[m](\phi, r_\phi + s)$. Note that $f_\phi(s) = 0$ for all $s \notin [0, D_\phi]$. When P is a differentiable point of C, since $\partial C(P)$ is a singleton, we may denote ℓ_{ϕ, r_ϕ} by ℓ_{θ_P, r_P} and f_ϕ by f_P.

All notations in definition 3.5 and 3.7 are shown in Figure 5.

Figure 5: Point P on C and its ℓ_{ϕ, r_ϕ}, $\ell_{\phi, r_\phi}^\perp$ and D_ϕ

Definition 3.8. We say that point P is a *locally linear* point on C if there is a neighborhood of P where C is a line in it.

Lemma 3.9. *For all $s \in (0, D_\phi)$, the line $\ell_{\phi, r_\phi + s}$ is intersects with C in exactly two points.*

Proof. Suppose that there is $s \in (0, D_\phi)$ such that the line $\ell_{\phi, r_\phi + s}$ is intersects with C in more than two points. If one point is isolated, we can draw a line connecting that point to the others as in Figure 6 (b). It belongs to A, which contradicts the convexity of A. If there is no isolated point, there is a part of C that intersects with $\ell_{\phi, r_\phi + s}$ which is locally linear as in Figure 6 (c). Since C is the boundary of the shape, one side of it should not be in A. Without loss of generality, we can suppose that it is the left side. We pick the point on that part of C which is farthest from $\ell_{\phi, r_\phi + s}$ so that the line connecting that point and P will not be contained in A. Again, this contradicts the convexity of A. So the only case that can happen is that it crosses only two points as shown in Figure 6 (a). □

Proposition 3.10. *The function f_ϕ is continuous and piecewise differentiable on $(0, D_\phi)$.*

Proof. By previous lemma, we have that the value of $f_\phi(s)$ on $(0, D_\phi)$ is equal to the distance between the two intersection points of $\ell_{\phi, r_\phi + s}$ and C. Since C is continuous on $(0, D_\phi)$, so is f_ϕ. We can also get piecewise differentiability of f_ϕ by a similar argument. □

Proposition 3.11. *The curve C is locally linear at P if and only if f_P is not continuous at 0.*

Proof. First of all, note that $\lim_{s \to 0^-} f_P(s) = 0$. Suppose that C is locally linear at P, then C is differentiable at P. So, $f_P(0)$ is equal to the length of C that intersect with ℓ_{θ_P, r_P}, which is greater than zero. That is f_P is not continuous at 0. On the contrary, suppose that C is not locally linear at P. So, C must intersect ℓ_{θ_P, r_P} only at point P, that is $f_P(0) = 0$. Since C is continuous, we get $\lim_{s \to 0^+} f_P(s) = 0$. This proves continuity of f_P at $s = 0$. □
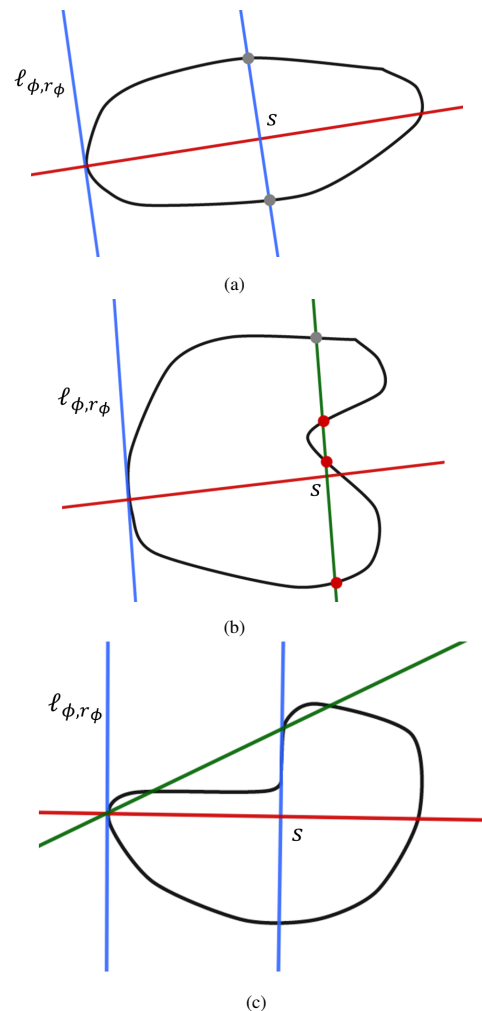

Figure 6: Non-differentiable point P on C and its ϕ^+, ϕ^-

Proposition 3.12. *If the curve C is differentiable at point P, then f_P is not differentiable at 0. Conversely, if f_ϕ is not differentiable at 0 for some $\phi \in \partial C(P)$, then C is differentiable at point P.*

Proof. Suppose that C is differentiable at P. Since ℓ_{θ_P, r_P} is tangent to C at P, we have $f'_P(0) = \infty$. On the contrary, suppose that C is not differentiable at P. There will be two distinct value $\phi^+ = \max\{\phi \in \partial C(P)\}$ and $\phi^- = \min\{\phi \in \partial C(P)\}$ as in Figure 7. Let $\phi \in \partial C(P)$. We get that $f'_\phi(s)$ will be bounded above and below by the slope of $\ell_{\phi^+, r_{\phi^+}}$ and $\ell_{\phi^-, r_{\phi^-}}$ evaluated with respect to ℓ_{ϕ, r_ϕ}. $\qquad \square$

Hence, by Remark 3.6, we can separate $\theta \in [-\pi, \pi)$ into three types according to the property of its corresponding point P as: a locally linear, a differentiable but not locally linear and a non-differentiable points. The Radon transform is discontinuous for the locally linear point, and the d-Radon transform is continuous but not differentiable. For the differentiable point that is not locally linear, the Radon transform is continuous but not differentiable, and the d-Radon transform is differentiable. Lastly, at the non-differentiable point, both Radon and d-Radon transform are differentiable.
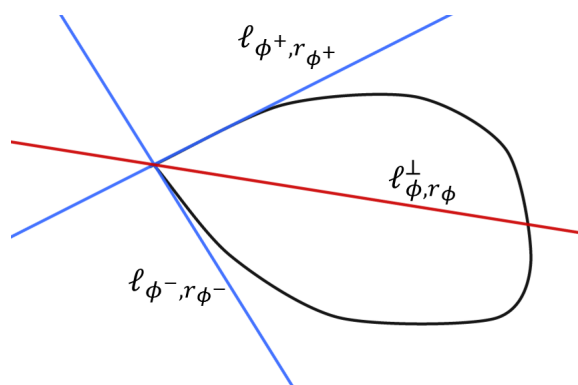

Figure 7: Non-differentiable point P on C and its ϕ^+, ϕ^-

To illustrated the result, take the following numerical examples.

Example 3.13. Consider a square

$$S = \{(x, y) : |x - y| + |x + y| \le 2\}.$$

Only the corner points $(-1, -1), (-1, 1), (1, -1)$ and $(1, 1)$ are non-differentiable points of S, and the others are locally linear. So, the Radon transform of S is not continuous only in the horizontal and vertical directions, see Figure 8. For d-Radon transform, it is continuous in every direction.
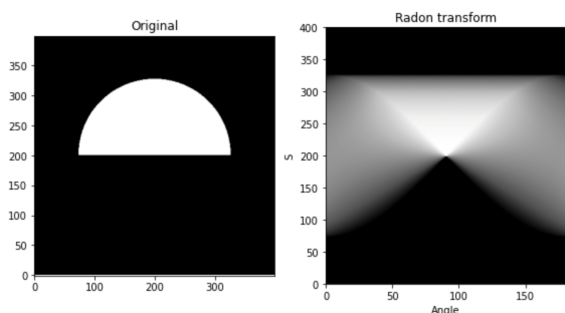

Figure 8: Image of the shape S in Example 3.13 and its Radon transform

Example 3.14. Consider a half circle

$$S = \{(x, y) : x^2 + y^2 \le 1, y \ge 0\}.$$

Only the corner points $(-1, 0)$ and $(1, 0)$ are non-differentiable points of S. All point on a base of the half circle is locally linear and the other are non-differentiable. So, the Radon transform of S is not continuous only in the horizontal direction, $\theta = 0$. For the other directions, the Radon transform is continuous, see Figure 9. Again, for d-Radon transform, it is continuous in every direction.
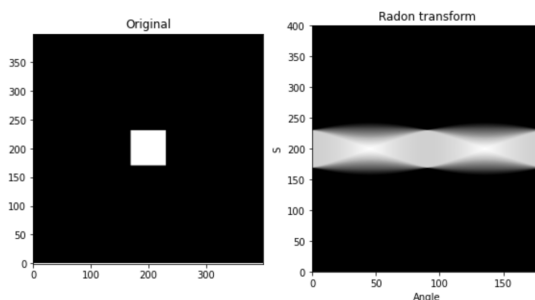

Figure 9: Image of the shape S in Example 3.14 and its Radon transform

4 Line Detection Methods

The line detection method is a procedure to indicate lines from a given image. In our setting, lines are parameterized by θ and r. So, line detection is a method to extract θ^{dt} and r^{dt} from each image. We can consider a line detection method as a set-valued function or correspondence that maps images to the set of detected parameters.

First, we consider the class $\mathfrak{B}_N$ of binary image consist of N circles on W. That is, $m \in \mathfrak{B}_N$ if $m : W \to \{0, 1\}$ in the form of

$$m(x, y) = \sum_{i=1}^{N} \delta_{B_{R_i}(P_i)} \qquad (16)$$

where $B_R(P)$ denotes a circle centered at P with radius R.

We define a distance between images $m_1, m_2 \in \mathfrak{B}_N$ that consist of circles $B_{R_i}(P_i)$ for $i = 1, ..., N$ and $B_{S_i}(Q_i)$ for $i = 1, ..., N$ respectively by: $\bar{D} : \mathfrak{B}_N \times \mathfrak{B}_N \to [0, \infty)$ as $\bar{D}(m_1, m_2) =$

$$\min_{\sigma \in \Pi_N} \sum_{i=1}^{N} \left(2 \min\{R_i, S_{\sigma(i)}\} \|P_i - Q_{\sigma(i)}\| + \pi |R_i^2 - S_{\sigma(i)}^2| \right)$$

where Π_N denotes the set of permutations of $\{1, 2, ..., N\}$ and $\|\cdot\|$ is the Euclidean norm on $\mathbb{R}^2$. It was shown in [1] that the function $\bar{D}$ is a distance function on $\mathfrak{B}_N$. This distance is a specific case of the Wasserstein metric.

For the set of points, if all points are located on the given line $r^* = x \cos \theta^* + y \sin \theta^*$, we get that $(\theta^*, r^*) = \text{argmax}_{(\theta, r) \in E} \mathcal{R}[m](\theta, r)$ []. We can extend this result to the image consist of circles.

Theorem 4.1. *Let $m \in \mathfrak{B}_N$ and $d > 0$. If the center of all circles in m are on the line $r^* = x \cos \theta^* + y \sin \theta^*$, we get that*

1. *$(\theta^*, r^*) = \text{argmax}_{\theta \in [-\frac{\pi}{2}, \frac{\pi}{2}]} \mathcal{R}[m](\theta, r)$,*

2. *$(\theta^*, r^*) \in \text{argmax}_{\theta \in [-\frac{\pi}{2}, \frac{\pi}{2}]} \mathcal{R}_d[m](\theta, r)$.*

In particular, if $d < R_i$ for all radius R_i of circle consisted in m, we get that $(\theta^*, r^*) = \text{argmax}_{\theta \in [-\frac{\pi}{2}, \frac{\pi}{2}]} \mathcal{R}_d[m](\theta, r)$.

The proof of this theorem can be found in [1]. The next step is to show the continuity of the *d*-Radon transform. Here, the maximum theorem is needed.

Lemma 4.2. *(Maximum Theorem, see Theorem 3.5 in [9]) Let X, Y to be topological spaces. For a continuous function $f : X \times Y \to \mathbb{R}$ and a compact value correspondence $C : Y \rightrightarrows X$ such that $C(y) \neq \emptyset$ for all $y \in Y$. Define a function $f^* : Y \to \mathbb{R}$ by $f^*(y) = \sup\{f(x, y) : x \in C(y)\}$ and a correspondence $C^* : Y \rightrightarrows X$ by $C^*(y) = \operatorname{argsup}\{f(x, y) : x \in C(y)\}$. If C is continuous at y, then f^* is also continuous at y and C^* is upper hemi-continuous at y.*

Theorem 4.3. *For $d > 0$ and $m \in \mathfrak{B}_N$. A correspondence $m \mapsto (\theta^{dt}, r^{dt})[m] = \operatorname{argmax}_{(\theta,r)\in E}\mathcal{R}_d[m](\theta, r)$ is upper hemi-continuous under the norm induced by metric $\bar{D}$.*

Proof. Let $d > 0$. Consider $\mathcal{R}_d$ as a function from $E \times \mathfrak{B}_N$ to $\mathbb{R}$ and a correspondence C defined by $C(m) = [-\frac{\pi}{2}, \frac{\pi}{2}]$ for all $m \in \mathfrak{B}_N$. To show that $\mathcal{R}_d$ is continuous, let $m_1, m_2 \in \mathfrak{B}_N$ and $(\theta_1, r_1), (\theta_2, r_2) \in E$. By linearity of the *d*-Radon transform, we have that

$$
\begin{aligned}
&|\mathcal{R}_d[m_1](\theta_1, r_1) - \mathcal{R}_d[m_2](\theta_2, r_2)| \\
&= |\mathcal{R}_d[m_1](\theta, r) - \mathcal{R}_d[m_1](\theta_2, r_2) \\
&\quad + \mathcal{R}_d[m_1](\theta_2, r_2) - \mathcal{R}_d[m_2](\theta_2, r_2)| \\
&\leq |\mathcal{R}_d[m_1](\theta, r) - \mathcal{R}_d[m_1](\theta_2, r_2)| \\
&\quad + |\mathcal{R}_d[m_1](\theta_2, r_2) - \mathcal{R}_d[m_2](\theta_2, r_2)|
\end{aligned}
$$

□

The last step follows from the fact that $\mathcal{R}_d$ is continuously differentiable. As a consequence, $\mathcal{R}_d : E \times \mathfrak{B}_N \to \mathbb{R}$ is continuous. Then, by maximum theorem, the correspondence $m \mapsto (\theta^{dt}, r^{dt})[m] = \operatorname{argmax}_{(\theta,r)\in E}\mathcal{R}_d[m](\theta, r)$ is upper hemi-continuous. So, if $\mathcal{R}[m]$ has a unique maximum, then a correspondence $m \mapsto (\theta^{dt}, r^{dt})[m] = \operatorname{argmax}_{(\theta,r)\in E}\mathcal{R}_d[m](\theta, r)$ is a continuous function.

Hence, we can extend this fact from an image consisting of circles to convex shapes. The main theorem can be restated as follows:

Theorem 4.4. *For $d > 0$ and image m consist of convex shape, if every point of edge of every shape in m are not locally linear, then correspondence $m \mapsto (\theta^{dt}, r^{dt})[m] = \operatorname{argmax}_{(\theta,r)\in E}\mathcal{R}_d[m](\theta, r)$ is upper hemi-continuous.*

Here, the metric used in this theorem is defined in the same way as $\bar{D}$ but on the image consists of convex shapes instead of circles.

5 Conclusion

The regularity of the Radon transform, its modification called the *d*-Radon transform, and line detection methods based on these two

transforms have all been investigated. The line detection method based on the Radon transform is not continuous for an image consisting of a circle. After more analysis, we determined that the circle has a differentiable edge at each point, which is the source of discontinuity. The locally linear point, differentiable point, and non-differentiable point are three types of shape edges. The Radon transform's regularity is determined by the sort of point on edge in that direction. A non-differentiable point is the only situation in which the Radon transformation can preserve its continuity. To achieve Radon transformation continuity in all directions, the shape must not be differentiable at all points, which is impossible.

To increase the regularity of the line detection method, we introduce the *d*-Radon transform by changing the domain of integration from line to strip. Equivalently, it integrates the Radon space in the *r* direction. The *d*-Radon transform of a convex shape was explored for regularity. We discovered that the differentiable requirement of the transformation is that the shape's edge is not locally linear. This is also a condition for the line detection method's continuity.

References

[1] P. Vatiwutipong, "Continuity of line detection methods based on the Radon transform," in 2022 14th International Conference on Knowledge and Smart Technology (KST), 29–33, 2022, doi:10.1109/KST53302.2022.9729056.

[2] J. Radon, "On the determination of functions from their integral values along certain manifolds," in IEEE Transactions on Medical Imaging, 170–176, 1986, doi:10.1109/TMI.1986.4307775.

[3] S. R. Deans, The Radon Transform and Some of Its Applications, Springer, 2007.

[4] S. R. Deans, "Hough Transform from the Radon Transform," IEEE Transactions on Pattern Analysis and Machine Intelligence, **2**, 185–188, 1981, doi: 10.1109/TPAMI.1981.4767076.

[5] G. T. Herman, Fundamentals of Computerized Tomography, Springer, 2009.

[6] M. C. B. M. P. A. M. M. Riccardo Aramini, Fabrice Delbary, "Hough Transform from the Radon Transform," arXiv:1605.09201, 2016, doi:10.48550/arXiv.1605.09201.

[7] C. L. Epstein, Introduction to the Mathematics of Medical Imaging, Society for Industrial and Applied Mathematics, 2009.

[8] T. G. Feeman, The Mathematics of Medical Imaging: A Beginner's Guide, Springer, 2015.

[9] N. S. P. Shouchuan Hu, Handbook of Multivalued Analysis 1: Theory, Springer, 1997.